Nanoscale

Accepted Manuscript

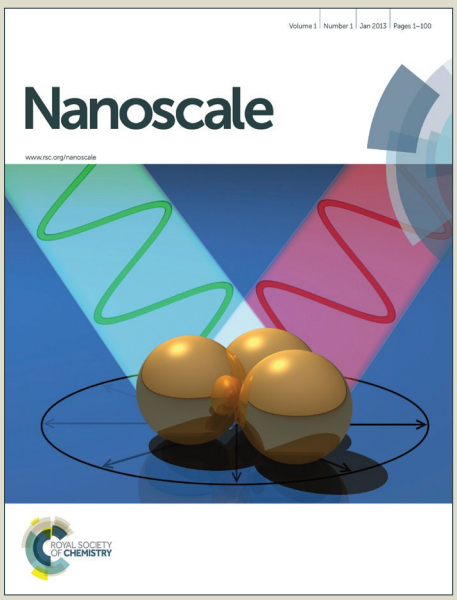

ROYAL SOCIETY OF CHEMISTRY

www.rsc.org/nanoscale

Nanoscale

ARTICLE

Received 00th January 20xx,

Accepted 00th January 20xx

DOI: 10.1039/x0xx00000x

www.rsc.org/

Below-gap excitation of semiconducting single-wall carbon nanotubes

G. Soavi,*[a,b] A. Grupp,[a] A. Budweg[a], F. Scotognella,[b,c,d] T. Hefner,[e] T. Hertel,[e] G. Lanzani,[d] A. Leitenstorfer,[a] G. Cerullo,[b,c] D. Brida†[a]

We investigate the optoelectronic properties of the semiconducting (6,5) species of single-walled carbon nanotubes b measuring ultrafast transient transmission changes with 20 fs time resolution. We demonstrate that photons with energ below the lowest exciton resonance efficiently lead to linear excitation of electronic states. This finding challenges th established picture of a vanishing optical absorption below the fundamental excitonic resonance. Our result points toward below-gap electronic states as an intrinsic property of semiconducting nanotubes.

1. Introduction

After more than two decades of intense research since their discovery,[1,2] carbon nanotubes still represent one of the most attractive systems for the study of physical phenomena in one dimension and a promising platform for advanced technology.[3,4] Single-wall carbon nanotubes (SWNTs) can be described as hollow cylinders obtained by rolling up a graphene sheet. A straightforward and rather precise approach to derive their electronic properties consists in applying the zone-folding scheme (i.e. circumferential periodic boundary conditions) to the electronic bands of graphene obtained by tight-binding (TB) calculations.[5] These boundary conditions are related to the folding geometry of the cylinder which is unambiguously defined by the chiral vector $\boldsymbol{C_h} = \boldsymbol{na_1} + \boldsymbol{ma_2}$. Here, $\boldsymbol{a_1}$ and $\boldsymbol{a_2}$ are the unit vectors of the graphene lattice.[6] From the pair of integers $(\boldsymbol{n}, \boldsymbol{m})$ it is also possible to predict whether a SWNT will be metallic or semiconducting,[5,6] with an energy gap scaling as the inverse of the tube diameter in the latter case.[7,8] This single-particle model has to be refined by considering many-body effects that lead to the formation of excitons,[9-12] bi-excitons[13,14] and trions.[15-17] In addition, a more detailed TB description of the electronic structure must take curvature into account, in particular at SWNT diameters below about 1 nm.[5,18-21] This effect is responsible for both the formation of a small band gap in metallic SWNTs[22] and a drastic reduction of the band gap in small-diameter semiconducting SWNTs.[23] Also defects, disorder and doping, including ambient contamination from water and oxygen during the synthesis, may strongly affect the electronic and transport properties of SWNTs.[24-26] Such extrinsic effects lead to phenomena like e.g. a plasma response in the THz frequency range,[27] local variations of the Fermi level[28] and the appearance of an Urbach tail in the effective density of states.[29] Finally, the intrinsic electronic properties of SWNTs may be modified by the presence of bundles which lead to lowering of the symmetry.[5] However, below-gap excitation in semiconducting SWNTs has been rarely investigated experimentally. In a previous study on HiPco (high-pressure carbon monoxide) SWNTs,[30] the obtained signal was assigned to thermal effects or to a non-resonant bleaching from large-diameter SWNTs. In another study, Song *et al.*[31] observed a long-lived bleaching of the S_{11} transition in a (6,5)-enriched sample which they attributed to weak excitation of real carriers through multiphoton absorption. On the other hand, absorption spectroscopy on individual and relatively large-diameter SWNTs hints to the presence of a "non-resonant" background with a cross-section comparable to the ideal graphene optical absorbance, regardless of the polarization (i.e. parallel or orthogonal to the tube axis) of the incident light.[32] Similarly, recent photoluminescence experiments showed a graphene-like wavelength-independent absorption at higher energy with respect to the S_{11} excitonic transition in small-diameter semiconducting SWNTs,[33] including the (6,5) chirality. In this work we apply ultrafast pump-probe spectroscopy to investigate the nature of excitations at low photon energy (i.e. below the fundamental gap) in small-diameter semiconducting SWNTs. We unambiguously show that optical excitation can occur below the excitonic gap *without exploiting non-linear processes* such as two-photon absorption. This result illustrates photo-physical phenomena in small-diameter semiconducting SWNTs beyond the conventional exciton physics. We suggest that significant theoretical and experimental efforts are still necessary to fully capture their energetic landscape.

2. Experimental

2.1 Sample preparation

[a] Department of Physics and Center for Applied Photonics, University of Konstanz, D-78457 Konstanz, Germany
[b] Dipartimento di Fisica, Politecnico di Milano, Piazza L. da Vinci 32, 20133 Milano, Italy
[c] IFN-CNR, Piazza L. da Vinci, 32, 20133 Milano, Italy
[d] Center for Nano Science and Technology@PoliMi, Istituto Italiano di Tecnologia, Via Giovanni Pascoli, 70/3, 20133 Milano, Italy
[e] Inst. for Physical and Theoretical Chemistry Dept. of Chemistry and Pharmacy, University of Würzburg, Würzburg 97074, Germany
* email: gs544@camn.ac.uk
† email: daniele.brida@uni-konstanz.de

The sample used for the experiments is highly enriched to contain a fraction of more than 80% of the (6,5) semiconducting species of SWNTs embedded in a gelatine film. It was prepared from 30 microliters of a density gradient ultracentrifugation-enriched (DGU) SWNT suspension in a sodium cholate (SC)/sodium dodecyl sulfate (SDS) mixture.[34] Iodixanol as well as SDS residues from the DGU process were removed by dilution with SC solution and filtration with a benchtop centrifuge. The resulting suspension was then mixed with 20 microliters of 15 wt% gelatine solution and finally drop-cast onto a thin glass substrate. The (6,5) chirality, characterized by a 0.75 nm diameter and a band gap of 1.26 eV, has been widely used to study the fundamental physical properties of semiconducting SWNTs.[17,28,35-38] This fact is mostly due to convenient spectroscopic access to the lowest subband exciton, abundance and ease of isolation if compared with other semiconducting species.[34,39]

2.2 Pump-probe experiments

Transient absorption spectroscopy was performed with a home-built system based on a 50-kHz Yb:KGW regenerative amplifier system (PHAROS, Light Conversion) that drives a tuneable IR optical parametric amplifier (OPA) delivering the pump pulses. As a probe we employ a white-light continuum (WLC) generated in a 4 mm sapphire plate. The pulses are compressed by means of a prisms pair (IR OPA) and by chirped mirrors (WLC), ensuring an overall temporal resolution of approximately 20 fs. The spectra of the three different pump pulses, obtained by tuning the IR OPA, are reported in Figure 1 together with the absorption spectrum of the (6,5) SWNT sample in the energy region of the first two excitonic transitions, S_{11} and S_{22}. The photon energies of the pump pulses (from 1 eV to 0.82 eV) are tuned to be well below the first S_{11} excitonic transition of the (6,5) SWNT at 1.26 eV. The probe pulse is spectrally resolved by a monochromator and lock-in detected by modulating the pump beam with a Pockels cell at 25-kHz frequency.

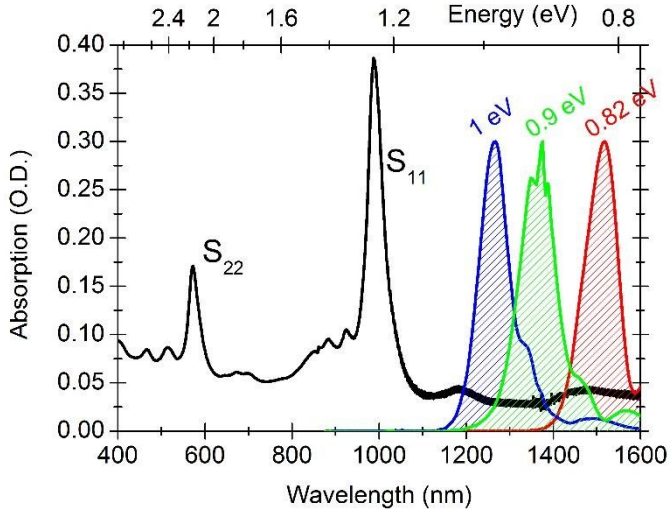

Fig. 1. Absorption spectrum of the (6,5) SWNT and the three pump pulses used in the pump-probe experiments. The first two excitons S_{11} and S_{22} reside at wavelengths of approximately 1 µm and 570 nm, respectively.

2.3 Transient spectra and coherent phonons

Figure 2 shows the measured differential transmission (ΔT/T) signal in the energy region of the S_{22} excitonic transition for excitation by photons with 0.9 eV energy. The results are similar for the three pump photon energies discussed in Fig. 1. Both the overall spectral shape and its ultrafast evolution (Fig. 2) strongly resemble the typical response of a (6,5) SWNT resonantly excited at the S_{11} transition,[40] despite the pump pulses in this study have much lower photon energy.

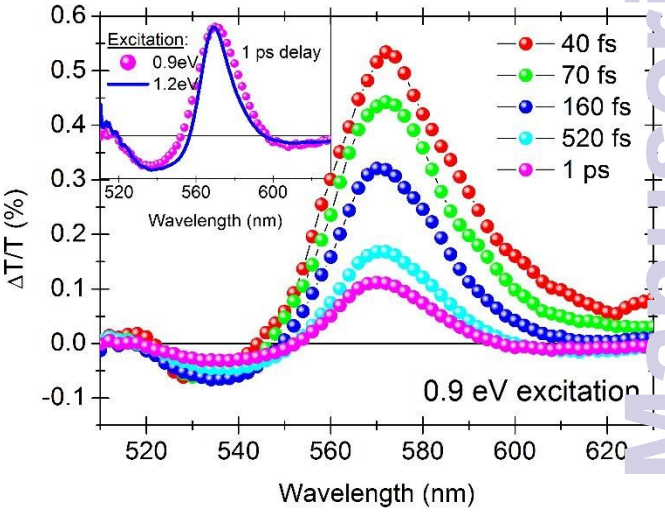

Fig. 2. Differential transmission signal ΔT/T at different pump-probe dela… the case of excitation at a photon energy of 0.9 eV. (inset) Comparis… between normalized ΔT/T signal for 0.9 eV (circles) and 1.2 eV excitation (blu… line), resonant with the S_{11} exciton, acquired at 1 ps pump-probe delay.

Figure 3a displays the ΔT/T dynamics monitored by probe pulse… 570 nm and 580 nm wavelength when the sample is excited wit… photons of 1 eV energy. The inset highlights that *the response of th… sample is instantaneous* within our temporal resolution of 20 fs. To… confirm that the sample is excited via a linear process, and thus t… exclude a two-photon excitation, we performed pump-probe… measurements as a function of the excitation fluence at the peak … the S_{22} bleaching (570 nm). Figure 3b demonstrates that the signal… scales linearly with the excitation over more than one order … magnitude, while Figure 4a shows a very weak dependence of the… decay constant on the pump fluence. The ΔT/T dynamics at 570 … probe wavelength is depicted in Fig. 4b as a function of the pump-… photon energy. The amplitude of the transient signal is virtually… independent of the photon energy of the pump pulse (see Figure 3b)… However, at higher pump photon energy the relaxation becomes… slightly faster, as it is typical for the thermalization processes … follow excitation within a continuum of states.[43] In addition, w… clearly observe that the dynamics of ΔT/T is always modulated by… periodic oscillations of the amplitude. The frequency of thes… oscillations of 310 cm^{-1}, as well as their modulation depth and phase… profile, allows us to ascribe them to an impulsively excited radi… breathing mode (RBM) of the (6,5) SWNT. In fact, the Fourier… amplitude of these coherent phonon oscillations vanishes at th… peak of the bleaching (see the dynamics at 570 nm probe wavelengt… in Figure 3a) and it exhibits maxima in its slopes (see the dynamics … 550 nm and 584 nm probe wavelengths in Figure 3c, respectively… with a clear jump in the phase by π between lower and higher prob… energies (Figure 3c).[44,45] Vibrational coherence can only b… established by an impulsive excitation occurring on a time scale Δt … τ where τ is the vibrational period of the specific mode. In our case… τ amounts to 110 fs. Off-resonance impulsive stimulated Raman

scattering is unlikely in a highly diluted sample where the matrix signal would vastly dominate. Also, it would not display the measured phase profile, with a phase jump by π around the excitonic resonance. In combination with the observation of a bleaching signal, our findings demonstrate that below-gap excitation creates a *real population of SWNT electronic states* by a dissipative process. This scenario is in stark contrast with coherent nonlinear interactions involving transient shifts of energy levels in the presence of a non-resonant light field as e.g. the optical Stark effect.[46] Such signals would last only for the temporal overlap of pump and probe pulses and would not cause a long-lived bleaching. Note that even the linear absorption spectrum of the sample, shown in Figure 1, displays a nearly featureless low-energy tail. While from linear absorption it is hard to discriminate the contributions of the SWNTs from that of the gelatine, scattering and impurities, our experiments clearly demonstrate that at least part of this absorption directly results from the intrinsic properties of the (6,5) SWNTs.

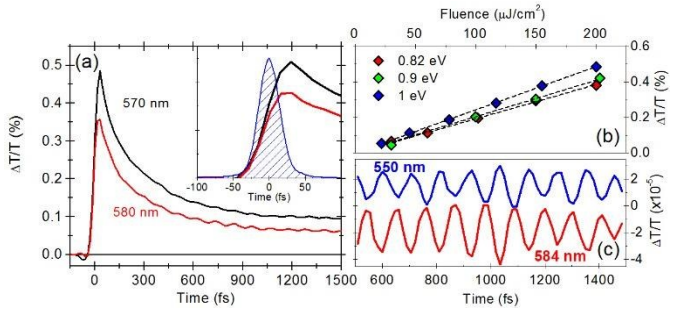

Fig. 3. (a) ΔT/T dynamics at 570 nm and 580 nm probe wavelengths. (inset) Zoom-in of the dynamics between -100 fs and 100 fs together with the auto-correlation of the pump pulse demonstrating a temporal resolution of approximately 20 fs. (b) Maximum amplitude of the pump-probe signal for the 570 nm probe wavelength as a function of the pump fluence and linear fits. (c) Coherent oscillations (assigned to the RBMs) detected at 584 nm (blue curve) and 550 nm (red curve) for 1 eV pump photon energy.

3. Results and discussion

Based on this experimental evidence, we now discuss the possible origin of the ΔT/T signal following low-energy optical excitation. (i) Since the pump photon energies are well below the S_{11} main peak transition energy, direct exciton photogeneration can be excluded. (ii) Another possibility is that excitons might be created via two-photon absorption with subsequent onset of exciton-exciton annihilation, resulting in linear fluence dependence. However, this scenario can be ruled out by considering that the photon energies employed in our experiments are not resonant with S_{11} via a two-photon transition. In addition, exciton-exciton annihilation can only occur at high densities of photoexcited states, which are extremely unlikely with our moderate pump fluences and assuming a two-photon absorption mechanism (Figure 3b). Finally, the amplitude of the S_{22} ΔT/Tsignal and the decay dynamics of the exciton bleaching should display non-linear dependence on the pump fluence,[38,47,48] which is not the case in our experiments as reported in Figure 4a. (iii) Thermal effects, for instance due to heating of the matrix, would not be instantaneous in the tube response and should persist on a timescale much longer than the ps decay we observe. In fact, heat transfer from the environment to the (6,5) SWNT would imply a rise-time of the signal in the picosecond range as typical for latt[illegible] heating dynamics.[49] (iv) Absorption of low-energy photons with th[illegible] corresponding annihilation of phonons is ruled out by the larg[illegible] tuning range of the pump pulses used in the experiments (which d[illegible] not match with any of the (6,5) SWNT phonons) and the negligib[illegible] population of high-energy phonons available at room temperature. To further exclude such phonon-assisted exciton generatio[illegible] mechanism, we have compared photoluminescence (PL) experiments following resonant S_{22} (2.17 eV) and below-gap (0.9 eV) excitation. The PL signal was collected at the peak of the S_{11} excito[illegible] (1.2 eV) in both cases. In these experiments we observed a clear and sharp PL signal in the case of S_{22} excitation while we did not observe any PL from below-gap excitation. (v) Our observation also rules ou[illegible] excitation and energy transfer from residual metallic or semiconducting tubes of other chiralities present in the sample, sinc[illegible] energy transfer from an unknown absorber to the (6,5) SWNT would be an unlikely up-hill event.

Fig. 4. (a) Fluence-dependent dynamics at 570 nm probe wavelength[illegible] Dynamics at 570 nm probe wavelength and 100 μJ/cm² pump fluence for the three different pump spectra used in the experiments. (inset) Comparison between dynamics after excitation off resonance at 0.82 eV (solid red line) and resonant pumping of the S_{11} exciton at 1.2 eV (circles) at a pump fluence of 60 μJ/cm². The ΔT/T signal for 0.82 eV excitation is multiplied by a factor of 20.

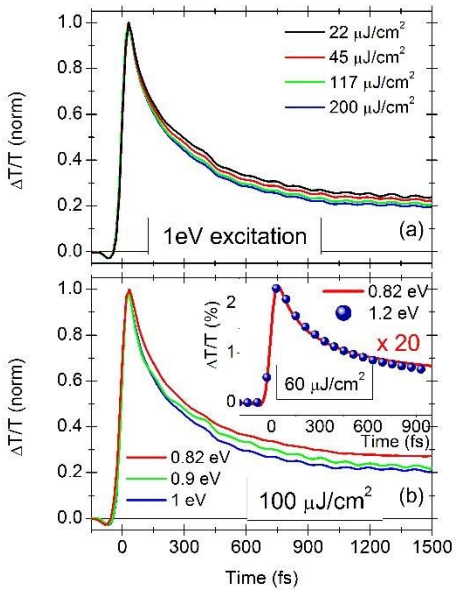

(vi) Finally, even in the case of unintentional p-doping of SWNTs, fo[illegible] instance due to interaction with the oxygen-water redox couple, absorption of light with polarization perpendicular to the tube axis might induce transitions between the S_{22} valence band and vacancies around the top of the S_{11} excitonic subband. We addressed this issu[illegible] by probing the first excitonic subband in the case of below-gap (0.9 eV) excitation. The results (Figure 5) show a clear bleaching signal from the S_{11} exciton, which again strongly resemble the case of resonant or above-gap excitation.[37] This allows us to exclude the aforementioned scenario, for which an increased absorption would be expected.

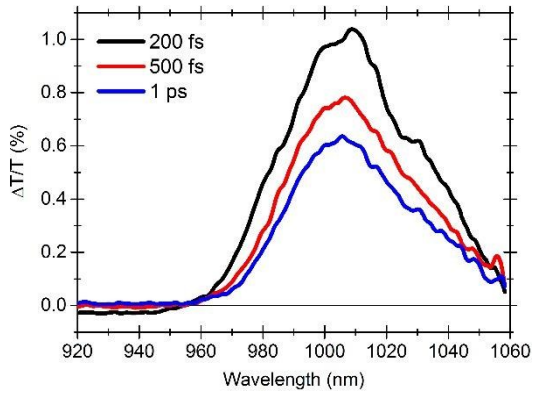

Fig. 5. ΔT/T spectra at different pump-probe delays in the energy region of the first S_{11} excitonic subband in the case of below gap (0.9 eV) excitation and ≈ 200 μJ/cm^2 fluence.

These experimental results allow us to assign the absorption of low-energy photons directly to linear excitation of the (6,5) SWNTs. The evidence that the amplitude of the signal does not depend on the pump photon energy (Figure 3b) further indicates that this excitation is associated with a distributed joint density of states directly related to the (6,5) SWNT. Similarly, since free charges are also strongly coupled to the RBMs of individual SWNTs,[50] the perturbation of the (6,5) electronic distribution can explain the presence of the coherent oscillations via electron-phonon coupling, without invoking excitonic effects. By comparing the ΔT/T signal amplitude in the case of resonant S_{11} (inset in Figure 2 and inset in Figure 4b) and resonant S_{22} excitation from ref. 35 with that of below-gap excitation, we are able to estimate a below-gap optical density (in the energy region between 0.8 and 1 eV investigated here) of approximately 0.07 – 0.012. Our experiments also indicate that below-gap excitation produces the same transient spectra (inset Figure 2 and Figure 5) and dynamics (inset Figure 4b) when compared to resonant excitation of the S_{11} transition. This result agrees with our previous studies,[42,51] where we show that the pump-probe signal is strongly affected by photo-generated free electron-hole pairs. In fact, the optical properties of SWNTs depend on the presence of optically excited or injected charges due to band-gap renormalization.[42,51-53] The influence of defects or doping[24-29] would result in shallow or deep traps:[26] the low energy of the pump photons and their broad tuning (from 1 eV to 0.8 eV) would require an extremely high and uniform level of doping which is unlikely with our sample quality. Nevertheless, we cannot firmly exclude the presence of such states and hopefully this work will trigger theoretical investigations in this direction. On the other hand, the nature of this below-gap continuum of electronic states may be intrinsic to the (6,5) SWNT and explained by the effect of finite curvature.[18] These findings might also explain some controversial observations such as the low photo-luminescence quantum yield in small diameter SWNTs[54] or linear charge photogeneration upon excitation in the energy region of the S_{11} exciton.[55,56]

Conclusions

In conclusion, our results unambiguously show that at frequencies below the well-known S_{11} singlet exciton resonance of SWNTs there exist transitions with non-negligible oscilla strength. Such transitions generate real population, causin state filling, bleaching of higher energy optical transitions an coherent phonons. These observations are consistent with a graphene-like electronic density of states that is associated to continuum in the spectral response. This fact may be describe by models including defects, doping or curvature effects an subsequent hybridization of orbitals at the tube surface. These results are thus challenging the commonly accepted picture fo the electronic structure of semiconducting SWNTs, warranting more refined theoretical descriptions that take into account e.g. deviations from linear geometry due to bending.

Acknowledgements

D.B. acknowledges the support of the Emmy Noether Program of the Deutsche Forschungsgemeinschaft (DFG), Zukunftskolleg and of EC through the Marie Curie CIG project "UltraQuEsT" no. 334463. C.G. and G.S. acknowledge support by the EC under Graphene Flagship (contract no. CNECT-ICT-604391). F.S., G.L. and T.H. acknowledge the ITN project 31663 "POCAONTAS". A.L. acknowledges the European Research Council Advanced Grant "UltraPhase" (ERC-2011-AdG no 290876).

Notes and references

1 S. Iijima, *Nature*, 1991, **354**, 56.
2 S. Iijima, and T. Ichihashi, *Nature*, 1993, **363**, 603.
3 R. H. Baughman, A. A. Zakhidov, and W. A. de Heer, Science, 2002, **297**, 787.
4 M. F. De Volder, S. H. Tawfick, R. H. Baughman, and A. J. Hart, *Science*, 2013, **339**, 535.
5 J.-C. Charlier, X. Blase, and S. Roche, Rev. Mod. Phys., 200 **79**, 677.
6 R. Saito, G. Dresselhaus, and M. S. Dresselhaus, *Physi Properties of Carbon Nanotubes* (Imperial college pres London, 1998)
7 C. White, and J. Mintmire, *Nature*, 1998, **394**, 29.
8 H. Kataura, Y. Kumazawa, Y. Maniwa, I. Umezu, S. Suzuki, Y Ohtsuka, and Y. Achiba, *Synth. Met.*, 1999, **103**, 2555.
9 T. Ando, *J. Phys. Soc. Jpn.*, 1997, **66**, 1066.
10 C. D. Spataru, S. Ismail-Beigi, L. X. Benedict, and S. G. Louie *Phys. Rev. Lett.*, 2004, **92**, 077402.
11 F. Wang, G. Dukovic, L. E. Brus, and T. F. Heinz, *Science*, 2005, **308**, 838.
12 J. Maultzsch, R. Pomraenke, S. Reich, E. Chang, D. Prezzi, A. Ruini, E. Molinari, M. Strano, C. Thomsen, and C. Lienau, *Phys Rev. B*, 2005, **72**, 241402.
13 T. G. Pedersen, K. Pedersen, H. D. Cornean, and P. Duclos, *Nano Lett.*, 2005, **5**, 291.
14 L. Colombier, J. Selles, E. Rousseau, J. Lauret, F. Vialla, C. Voisin, and G. Cassabois, *Phys. Rev. Lett.*, 2012, **109**, 197402
15 T. Rønnow, T. Pedersen, and H. Cornean, *Phys. Rev. B* 2010, **81**, 205446.
16 K. Watanabe, and K. Asano, *Phys. Rev. B*, 2012, **85**, 035416.
17 S. M. Santos, B. Yuma, S. Berciaud, J. Shaver, M. Gallart, P Gilliot, L. Cognet, and B. Lounis, *Phys. Rev. Lett.*, 2011, **107** 187401.

18 X. Blase, L. Benedict, E. Shirley, and S. Louie, *Phys. Rev. Lett.*, 1994, **72**, 1878.
19 A. Kleiner, and S. Eggert, *Phys. Rev. B*, 2001, **64**, 113402.
20 V. Zólyomi, and J. Kürti, *Phys. Rev. B*, 2004, **70**, 085403.
21 I. Cabria, J. Mintmire, and C. White, *Phys. Rev. B*, 2003, **67**, 121406.
22 M. Ouyang, J. L. Huang, C. L. Cheung, and C. M. Lieber, *Science*, 2001, **292**, 702.
23 Y. Matsuda, J. Tahir-Kheli, and W. Goddard, *J. Phys. Chem. Lett.*, 2010, **1**, 2946.
24 D. Kang, N. Park, J. Ko, E. Bae, and W. Park, *Nanotechnology*, 2005, **16**, 1048.
25 P. G. Collins, K. Bradley, M. Ishigami, and A. Zettl, *Science*, 2000, **287**, 1801.
26 S. Lee, G. Kim, H. Kim, B.-Y. Choi, J. Lee, B. W. Jeong, J. Ihm, Y. Kuk, and S.-J. Kang, *Phys. Rev. Lett.*, 2005, **95**, 166402.
27 Q. Zhang, E. H. Hároz, Z. Jin, L. Ren, X. Wang, R. S. Arvidson, A. Lüttge, and J. Kono, *Nano Lett.*, 2013, **13**, 5991.
28 S. Schafer, N. B. Cogan, and T. D. Krauss, *Nano Lett.*, 2014, **14**, 3138.
29 D. Jones, and J. Lee, *Nano Lett.*, 2011, **11**, 4176.
30 R. Ellingson, C. Engtrakul, M. Jones, M. Samec, G. Rumbles, A. Nozik, and M. Heben, *Phys. Rev. B*, 2005, **71**, 115444.
31 D. Song, F. Wang, G. Dukovic, M. Zheng, E. D. Semke, L. E. Brus, and T. Heinz, *Appl. Phys. A*, 2009, **96**, 283.
32 J.-C. C. Blancon, M. Paillet, H. N. Tran, X. T. Than, S. A. Guebrou, A. Ayari, A. S. Miguel, N.-M. M. Phan, A.-A. A. Zahab, J.-L. L. Sauvajol, N. D. Fatti, and F. Vallée, *Nat. Commun.*, 2013, **4**, 2542.
33 F. Vialla, E. Malic, B. Langlois, Y. Chassagneux, C. Diederichs, E. Deleporte, P. Roussignol, J.-S. Lauret, and C. Voisin, *Phys. Rev. B*, 2014, **90**, 155401.
34 J. Crochet, M. Clemens, and T. Hertel, *J. Am. Chem. Soc.*, 2007, **129**, 8058.
35 J. R. Schneck, A. G. Walsh, A. A. Green, M. C. Hersam, L. D. Ziegler, and A. K. Swan, *J. Phys. Chem. A*, 2011, **115**, 3917.
36 J. Blackburn, J. Holt, V. Irurzun, D. Resasco, and G. Rumbles, *Nano Lett.*, 2012, **12**, 1398.
37 Z. Zhu, J. Crochet, M. S. Arnold, M. C. Hersam, H. Ulbricht, D. Resasco, and T. Hertel, *J. Phys. Chem. C*, 2007, **111**, 3831.
38 L. Lüer, S. Hoseinkhani, D. Polli, J. Crochet, T. Hertel, and G. Lanzani, *Nat. Phys.*, 2009, **5**, 54.
39 S. Bachilo, L. Balzano, J. Herrera, F. Pompeo, D. Resasco, and R. Weisman, *J. Am. Chem. Soc.*, 2003, **125**, 1186.
40 J. Park, P. Deria, and M. J. Therien, *J. Am. Chem.Soc.*, 2011, **133**, 17156.
41 J. Crochet, S. Hoseinkhani, L. Lüer, T. Hertel, S. Doorn, and G. Lanzani, *Phys. Rev. Lett.*, 2011, **107**, 257402.
42 G. Soavi, F. Scotognella, D. Brida, T. Hefner, F. Späth, M. Antognazza, T. Hertel, G. Lanzani, and G. Cerullo, *J. Phys. Chem. C*, 2013, **117**, 10849.
43 G. Della Valle, M. Conforti, S. Longhi, G. Cerullo, and D. Brida, *Phys. Rev. B*, 2012, **86**, 155139.
44 Y.-S. S. Lim, K.-J. J. Yee, J.-H. H. Kim, E. H. Hároz, J. Shaver, J. Kono, S. K. Doorn, R. H. Hauge, and R. E. Smalley, *Nano Lett.*, 2006, **6**, 2696.
45 L. Lüer, C. Gadermaier, J. Crochet, T. Hertel, D. Brida, and G. Lanzani, *Phys. Rev. Lett.*, 2009, **102**, 127401.
46 T. Unold, K. Mueller, C. Lienau, T. Elsaesser, and A. D. Wieck, *Phys. Rev. Lett.*, 2004, **92**, 157401.
47 L. Valkunas, Y.-Z. Ma and G. R. Fleming, *Phys. Rev. B*, 2006, **73**, 115432.
48 F. Wang, G. Dukovic, E. Knoesel, L. E. Brus, T. F. Heinz, *Phys. Rev. B*, 2004, **70**, 241403(R).
49 G. V. Hartland, *Chem. Rev.*, 2011, **111**, 3858.
50 B. J. LeRoy, S. G. Lemay, J. Kong, and C. Dekker, *Nature*, 2004, **432**, 371.
51 G. Soavi, F. Scotognella, D. Viola, T Hefner, T. Hertel, G. Cerullo and G. Lanzani, *Sci. Rep.*, 2015, **5**, 9681.
52 M. Steiner, M. Freitag, V. Perebeinos, A. Naumov, J. P. Small A. A. Bol and P. Avouris, *Nano Lett.*, 2009, **9**, 3477.
53 W. J. Kennedy and Z. V. Vardeny, *Appl. Phys. Lett.*, 2011, **98**, 263110.
54 P. Avouris, M. Freitag, and V. Perebeinos, *Nature Photonics*, 2008, **2**, 341.
55 M. Beard, J. L. Blackburn, and M. Heben, *Nano Lett.*, 2008, **8**, 4238.
56 S. A. Jensen, R. Ulbricht, A. Narita, X. Feng, K. Müllen, T. Hertel, D. Turchinovich, and M. Bonn, *Nano Lett.*, 2013, **13**, 5925.